95   10   24

4 10

( )　　　　　　　　　　http //www.nsc.gov.tw
( )　　　　　　　　(keywords)
( )

A4

( )　　　　　　　　　　　　　　　I　II　III
　　　　　　　　　　　　　　　　1.2.3.
( )
( )

( )

1.
　　　　A4　　　　　29.7　　　　21
2.
Single Space
3.
Times New
　Roman Font　　　　　　　　　　　　　　　　12

(　　　　　　　　)

95　　　　10　　　31

Abstract

Using porous anodic aluminum oxide as template and petroleum pitch as precursor, a massive amount of uniform carbon nanofibers was obtained after thermal treatment. The diameter and length were 300 nm and 60 μm respectively. The difference between these and the classic herringbone structure is that the angle between the graphenes and the fiber axis increases regularly along the axis instead of being fixed. TEM observations show that the nanofiber consists of stacked conical graphenes with cone angles that steadily increase from 60° to 180° along the fiber axis. This structure is the first to be produced without using catalytic CVD, and has not been reported using template procedures. The large deformation of the grapheme planes at the tip of the nanofiber may produce interesting electronic applications.

1. Introduction

Nanoscale carbon materials have attracted great interdisciplinary attention for the development of novel applications. due to their unique anisotropic properties By conventional catalytic CVD , diverse one-dimensional carbon nanoforms have been successfully synthesized, but avoiding encapsulating the metal catalyst into the product is a major obstacle. Recently, the technique of using porous oxide as the template in the synthesis of carbon nanomaterials has progressed rapidly. The template method has many significant advantages such as its non-residual catalysts, morphological controllability, microstructure, and the electrically conducting behavior of the product can even be manipulated by utilizing the anchoring effect. Recent works indicate that when using polycyclic aromatic hydrocarbons (PAHs) as precursor, relatively highly graphitized carbon nanomaterials can be obtained, whereas an amorphous microstructure will be formed by choosing an olefin as the carbon source. There are two types of anchoring, edge-on and face-on, which influence the arrangement of graphenes inside the product. All reported products from various PAHs precursors have the same characteristic, with the orientation of graphenes tending to be perpendicular to the long axis. The results are fully consistent with the edge-on anchoring effect.

Here we report a herringbone-type carbon nanofiber, built from a stack of conical graphenes which is obtained by this template method. The current herringbone-type carbon nanoforms are always synthesized by the catalytic CVD method, with the orientation of the graphenes incline to the long axis at approximately fixed angle. The difference between the classical herringbone structure and our nanofiber is that the orientation of the graphenes with respect to the fiber axis changes constantly in our product. Usually this type of carbon form has a tapered end, and in theory this end possesses localized states at the Fermi level which may exhibit unusual electronic properties. Herringbone-type nanomaterials have the potential to develop novel electronic devices, field emission sources and electrode materials.

2. Experimental

The precursor is isotropic petroleum pitch (A-240, Ashland Inc.) composed of hetero-polycyclic aromatic hydrocarbons units. The template is the commercial porous anodic alumina (from Whatman Ltd.). A holder with four cylindrical concavities is used to support the template and the powdered pitch. The powdered precursor is placed on the template. After inserting the holder into a tube furnace, the temperature was held at 300 ^{o}C for a half hour in

flowing Ar to soften the precursor. The liquid phase pitch was pulled into the channels by capillary attraction. Afterward it was gradually raised to 700 ^{o}C in 2h for the pyrolysis process, and then the system was cooled down naturally. The template was removed by immersing in 48 % hydrofluoric acid for 12h. The residual sample was washed and then oven-dried at 120 ^{o}C. The high-temperature treatment was performed by a graphitization furnace with a maximal temperature of 2500 ^{o}C. The experimental process is illustrated in figure S3. The products were characterized by scanning electron microscope (SEM, JEOL JSM-6500F at 15 kV) and high-resolution transmission electron microscope (HRTEM, JEOL JEM-2010 and Philips TECNAI 20 at 200 kV). The qualitative analyses were performed by using X-ray diffractometry (XRD, Shimadzu XRD-6000) and Raman spectroscopy (JOBIN YVON T64000).

3. Results and Discussions

The sample used for studying the structure details was synthesized at 700 ^{o}C and graphitized at 2500 ^{o}C. The degree of graphitization was identified by XRD, as shown in figure 1a. When the treatment temperature was under 1000 ^{o}C, the major peaks of the products at around $2\theta = 26$, 42 and 44° were assigned to the (002), (100) and (101) planes of bulk graphite. After treating at 1500 or 2500 ^{o}C, the intensity of the peak at 26° became notably stronger. Compared with the intensity of the (002) plane, the diffraction due to the (100) and (101) planes are almost invisible. Simultaneously two more peaks developed at 54 and 77°, which are assigned to the (004) and (110) planes respectively. The graphitization can also be quantified by the I_D/I_G ratio from Raman spectroscopy, as shown in figure 1b. The I_D/I_G ratio of the graphitized product is 0.251, which is lower than that of conventional multi-walled CNTs ($I_D/I_G = 0.86$).

The treated product was examined by electron microscope. After pyrolysis at 700 ^{o}C, the products were composed of bundles of fibers, as shown in figure 2a. The diameter and length of these bundles were around 300±50 nm and 60 μm, respectively. The inset in figure 2a demonstrates that some fibers could be bent to 180°, suggesting flexibility. The dimensions of the product correspond to the channel size of the template, implying that the liquid phase pitch was completely pulled into the channels by capillarity. From figure 2b, the top-view image of the inset, the product seems to be tubular. But it actually has a solid interior with a concave end indicated by the arrow; thus the product should be regarded as a fiber. The carbon yield of the pitch pyrolysis reaction is about 46%. The formation mechanism of the concave end is ascribed to the higher capillary affinity between the surface of the template and the liquid phase pitch. After treating at 2500 ^{o}C, the structure became fragile and easily fragmented (figure 2c), therefore nanofibers with full length up to 60 μm were difficult to find in the graphitized sample. The EDS analysis revealed that the precursor contained small amount of sulfur which could be driven out by heating above 2000 ^{o}C.

Recent work reports that the surface anchoring states between liquid-crystalline PAHs and substrates dominate the microstructure of the resultant carbon materials. When examining the as-pyrolyzed products by HRTEM, the graphenes of the nanofiber could be observed to incline to the fiber axis (figure 2d). Even after graphitization this tendency remained unchanged (figure 2e). The orientational pattern agrees with the description of the edge-on anchoring effect. Following graphitization treatment at 2500 ^{o}C, some closed loops constructed of 4~5 curled graphitic layers on the very edge of the nanofiber appeared, as shown in figure 2e. The surface energy of the graphenes tends to be reduced by forming loops, which are more stable than open edges at high

temperature. These closed ends are disadvantageous for developing applications utilizing active sites, but these can be created by oxidizing the samples in air flow at 600 ^{o}C for 2h. The interlayer spacing between each graphene sheet is 0.342 nm, which is slightly larger than in graphite owing to the imperfect stacking of turbostratic graphenes. The diffraction patterns are shown in the insert. Figure 2f presents an oblique cross-sectional view which implies that the nanofiber was amorphous, which agrees with the observation mentioned above. In contrast, the cross-section of conventional crystalline CNT-like structures reveals manifest concentric circles.

Because the nanofibers easily break into a mass of fragments after graphitization treatment, the lattice images of one fragment were investigated thoroughly. A typical fragment had a tapered and a funnel-shaped end with differing inclinations. The angle at the convex tip (labeled **1)** was always slightly larger than the angle in the concave end (labeled **2)**, as shown in figure 3c. According to figure 3, the graphenes in the microstructure are not normal to the fiber axis. Along the fiber axis, the inclinations are measured to be 99° (labeled **b**), 112° (**c**) and 157° (**d**). Thus the orientation of inclined graphenes changes uniformly from one end to the other. In figure 3a, mirror symmetry across the central axis composed of two groups of inclined graphenes is obvious. Combining the studies of the contours and the microstructure of the fragment, we can reason that the angles of the truncated ends are directly related to the inclination of the graphenes. For example, the angle (labeled **1**) measured in TEM is similar to the angle (labeled **a)** measured in the lattice image. Sometimes a thin amorphous carbon sheath coating the fragments might be observed. It is attributed to the adhesion of carbonaceous impurities during the experimental process and can be removed by oxidization in air flow at 500 ^{o}C for 2h.

The stacking can also be observed by electron diffraction patterns in the TEM. According to figure 4a, where the selected area is focused on the very edge of the nanofiber, only one group of (002) diffraction spots appear, whereas when focused on the center, two rows of (002) single crystal spots can be seen. The cross angles between the two sets of (002) diffraction spots relate to the arrangement of graphitic laminations in the microstructure. This signifies that the framework of the fragment is symmetrical about the central axis, composed of two groups of single crystalline graphitic laminations. Figure 4b and 4c indicate that the inclination of the diffraction patterns coincides with the shape of the truncated end. After surveying many fragments with their respective diffraction patterns, the range of the inclinations was determined to be between 60° and 180°. Thus the logical conclusion is that the carbon nanofiber consists of two groups of inclined graphitic laminations of angles between 60° and 180°.

So the microstructure of the carbon nanofiber can be identified as herringbone-type graphite. To consider the three-dimensionally cylindrical contour, the conventional herringbone structured fibers can be regarded as assembled from stacking conical graphenes with fixed cone angles. But our nanofiber has the unique characteristic that the angle between the graphenes and fiber axis increases regularly. In other words, the nanofiber is assembled from stacking conical graphenes with progressively varied cone angles. The different angles were attributed to the different aromatic rings added on the tip of the cone. The varying morphology is attributed to both the edge-on anchoring effect and the capillary affinity. At the ends, the angles between the graphene and the axis are created by the meniscus of the liquid phase pitch in the channels due to surface tension as injecting water into a capillary tube, whereas in the middle of the channel the edge-on effect will dominate resulting in the graphene becoming normal to the axis. After thermal

treatment the conical stacking was formed for minimizing the total energy because the conical shape has maximum sp^2 bonding which is more stable in high temperature. Figure 4d illustrates the stacking form.

4. Conclusions

A novel type of herringbone-type carbon nanofiber constructed by stacking graphitic nanocones with different cone angles has been successfully synthesized. The average diameter is 300 nm, the full length 60 μm and the range of cone angle varies continuously from 60° to 180° along the fiber. The morphology implies that the spacing between graphitic planes gradually becomes narrower from periphery to the centre. The morphology and microstructure of the nanofiber can be controlled based on the surface affinity between template and the precursor. The nanofiber might be developed for applications such as storage media, anodes in lithium-ion cells and novel electronic devices.
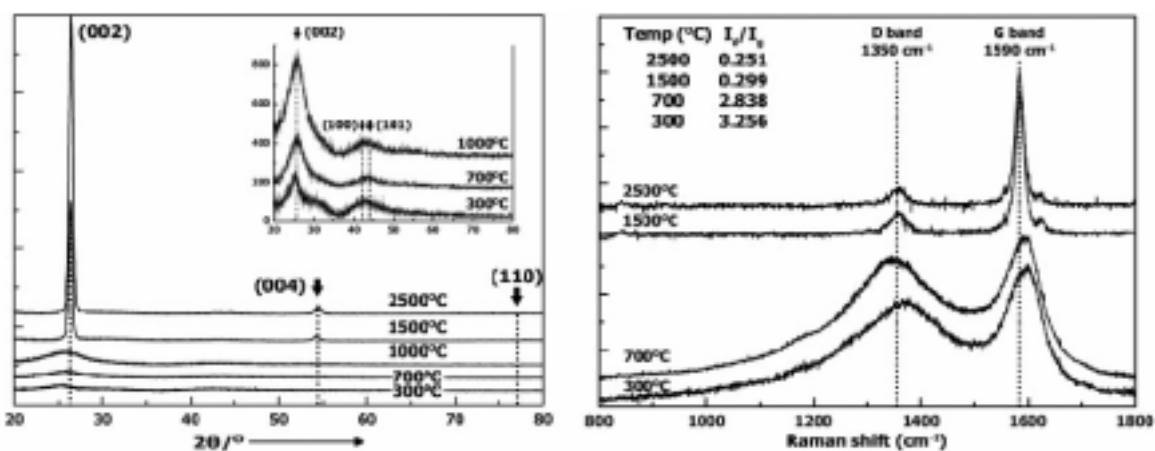

Figure 1.a) X-ray diffraction pattern and b) Raman spectrum for thermally treated samples. The inset in figure 1a is an expanded plot showing fibers related to different pyrolysis temperatures.
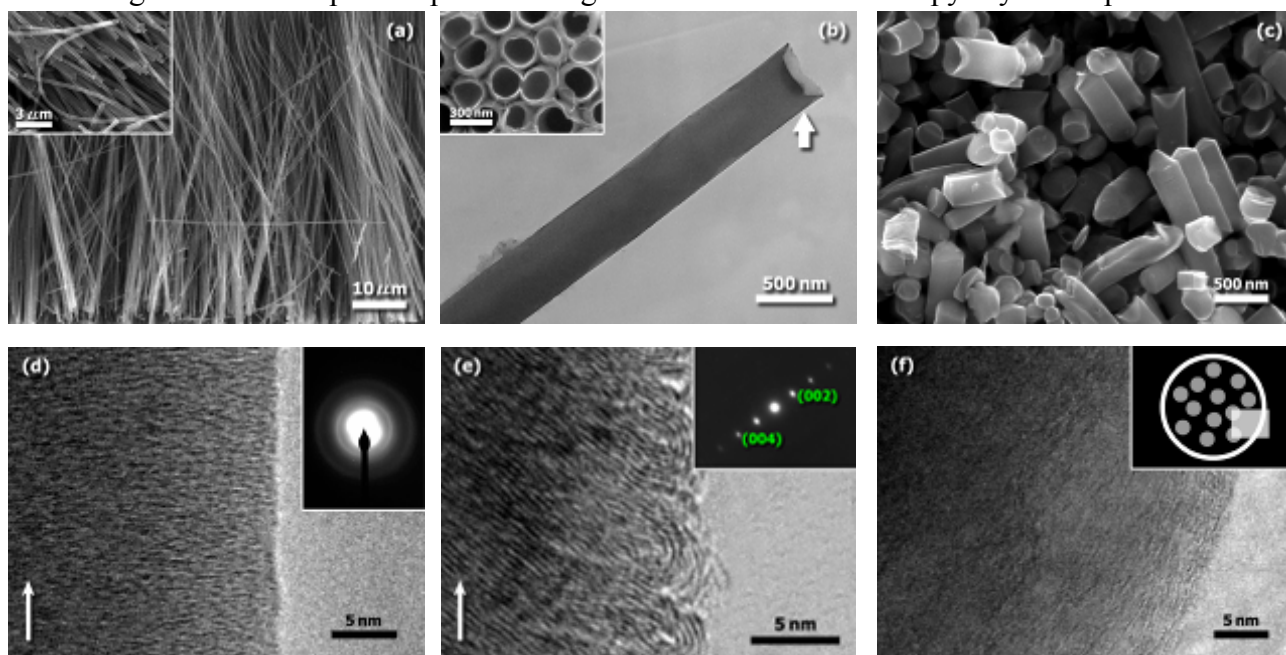

Figure 2. Morphologies and microstructural studies of the products: a) SEM and b) TEM image of fibers treated at 700 ^{o}C. The inset is the top-view SEM image. c) SEM image of the sample after 2500 ^{o}C treatment. d) Lattice image of the nanofiber treated at 700 ^{o}C and e) treated at 2500 ^{o}C showing that the graphene planes are inclined to the fiber axis (arrow). The diffraction pattern

represents the (002) planes of bulk graphite. f) Cross-sectional image of the sample treated at 2500 °C showing that it is amorphous. The inset shows the selected area viewed from a transverse plane.
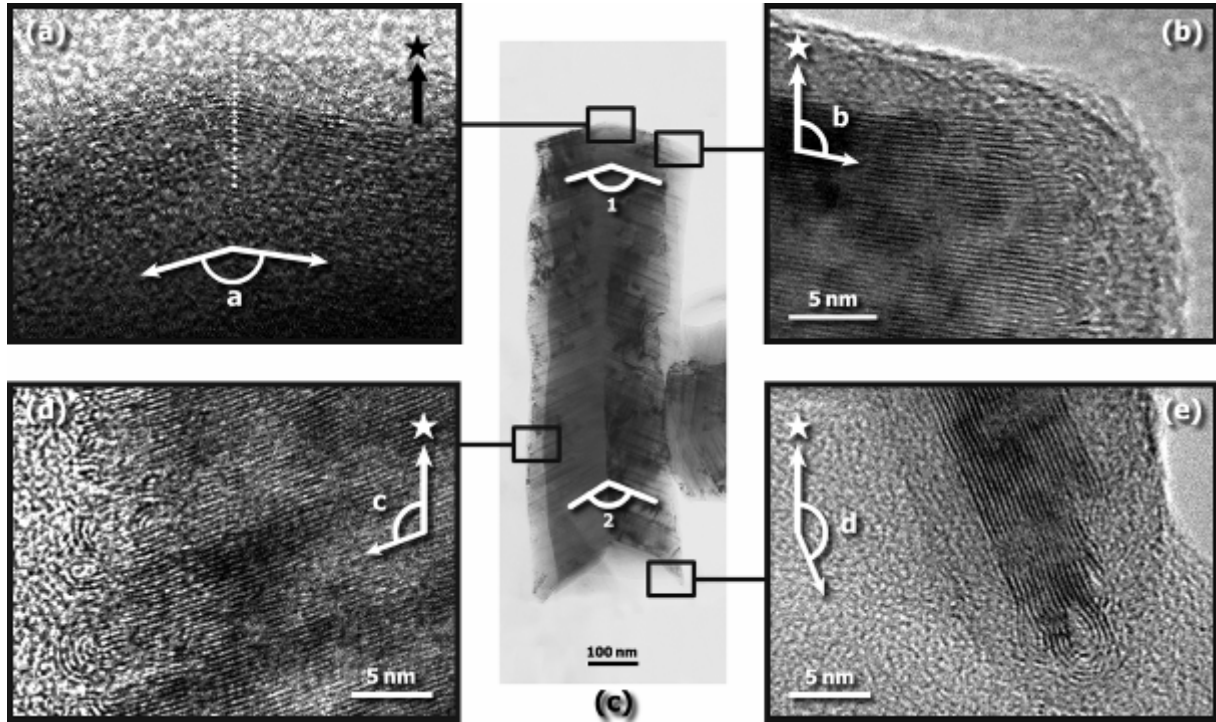
Figure 3. Lattice images a of single carbon fragment: a) a convex end exhibits the mirror symmetry of both sets of graphenes planes. b) Lattice image of an edge. c) TEM image of a fragment. d) Image of a shoulder. e) Image of the concave end. The arrow with a star indicates the direction of the fiber axis.
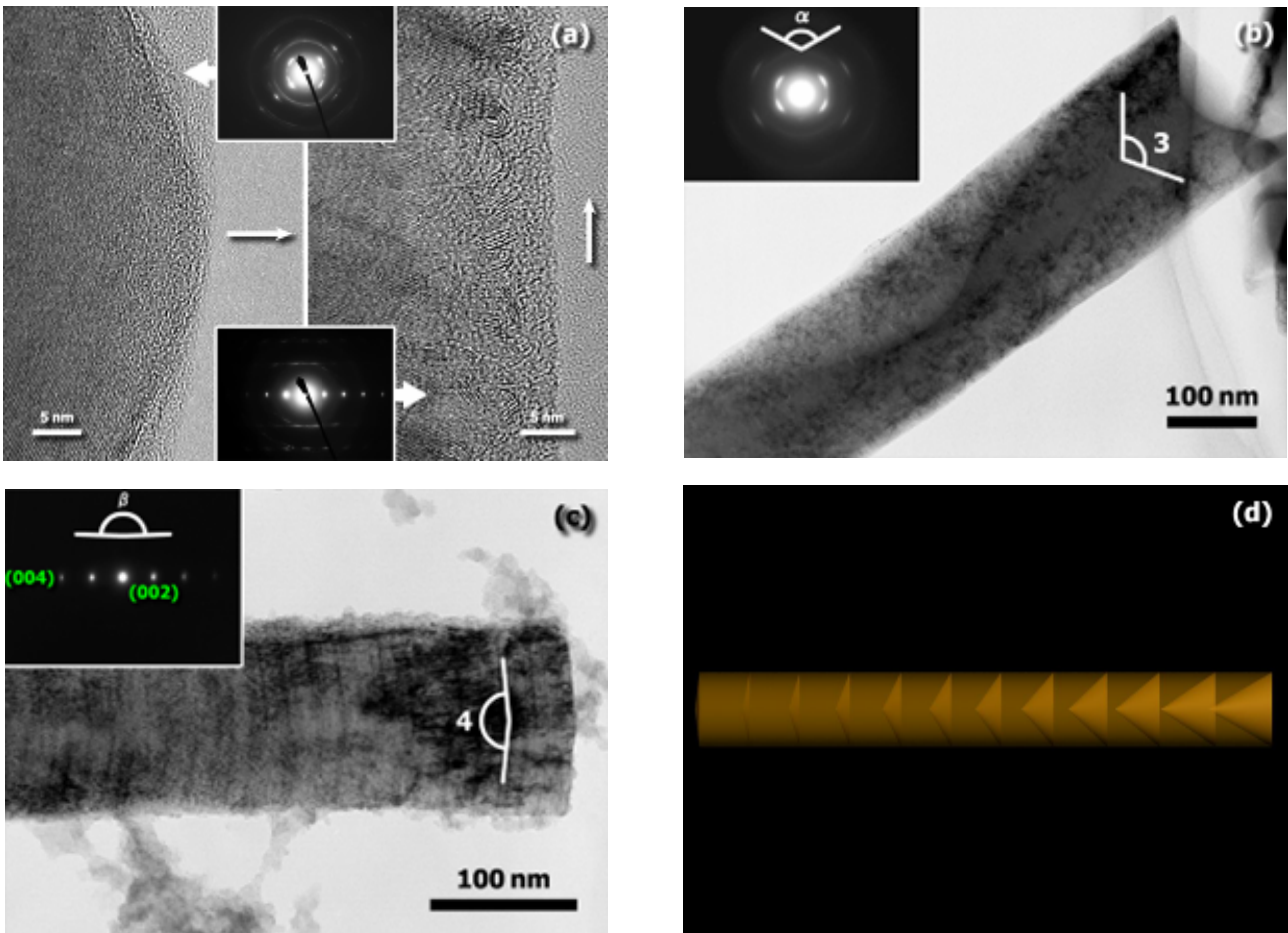
Figure 4. Studies of the correlation between the microstructures and diffraction patterns: a) Pattern focused on the centre of the fiber (left) showing a pair of (002) planes and one series of (002) spots as focused on the edge side (right). b) TEM image of the nanofiber. The angle of concave end (labeled **3**) is similar to the angle (labeled **α**) in the diffraction pattern (inset). And the angle of convex end (labeled **4**) is similar to the angle (labeled **β**) in the diffraction pattern (inset). d) Scheme illustrating the microstructure of the nanofiber.

可供推廣之研發成果資料表

／	
／	
	100~500

1.

2

3.